HAL open science

Impacts of metallic trace elements on an earthworm community in an urban wasteland: Emphasis on the bioaccumulation and genetic characteristics in Lumbricus castaneus

Helene Audusseau, Franck Vandenbulcke, Cassandre Dume, Valentin Deschins, Maxime Pauwels, Agnès Gigon, Matthieu Bagard, Lise Dupont

To cite this version:

Helene Audusseau, Franck Vandenbulcke, Cassandre Dume, Valentin Deschins, Maxime Pauwels, et al.. Impacts of metallic trace elements on an earthworm community in an urban wasteland: Emphasis on the bioaccumulation and genetic characteristics in Lumbricus castaneus. Science of the Total Environment, 2020, 718, pp.137259. 10.1016/j.scitotenv.2020.137259 . hal-02930066

HAL Id: hal-02930066

https://hal.inrae.fr/hal-02930066v1

Submitted on 7 Mar 2022

HAL is a multi-disciplinary open access archive for the deposit and dissemination of scientific research documents, whether they are published or not. The documents may come from teaching and research institutions in France or abroad, or from public or private research centers.

L'archive ouverte pluridisciplinaire **HAL**, est destinée au dépôt et à la diffusion de documents scientifiques de niveau recherche, publiés ou non, émanant des établissements d'enseignement et de recherche français ou étrangers, des laboratoires publics ou privés.

Distributed under a Creative Commons Attribution - NonCommercial 4.0 International License

Version of Record: https://www.sciencedirect.com/science/article/pii/S0048969720307695
Manuscript_ccb87033487357b186bb8cff1341af65

Impacts of metallic trace elements on an earthworm community in an urban wasteland: emphasis on the bioaccumulation and genetic characteristics in *Lumbricus castaneus*

Hélène Audusseau [1,2,3*], Franck Vandenbulcke [4], Cassandre Dume [1,4], Valentin Deschins [1], Maxime Pauwels [5], Agnès Gigon [1], Matthieu Bagard [1] and Lise Dupont [1]

1. Univ. Paris Est Creteil, Sorbonne Université, CNRS, INRA, IRD, Institut d'écologie et des sciences de l'environnement de Paris, 94010 Créteil, France
2. Department of Zoology, Stockholm University, Stockholm, Sweden
3. UK Centre for Ecology & Hydrology Maclean Building, Benson Lane, Wallingford, Oxon, OX10 8BB, UK.
4. Université de Lille, EA 4515-LGCgE - Laboratoire Génie Civil et géo-Environnement, Cité scientifique, SN3, F-59655 Villeneuve d'Ascq, France
5. Université de Lille, CNRS, UMR 8198 – Unité Evolution-Ecologie-Paléontologie, F-59000 Lille, France

* Corresponding author; e-mail address: helene.audusseau@zoologi.su.se

© 2020 published by Elsevier. This manuscript is made available under the CC BY NC user license
https://creativecommons.org/licenses/by-nc/4.0/

19 **Highlights**

20 Impact of soil pollution on earthworms at different levels of biological organisation.

21 Differential effects of MTEs on earthworms were investigated in an urban wasteland.

22 Community structure and *L. castaneus* physiology and genetics were studied.

23 MTEs affected earthworm community and bioaccumulation, but not population genetic.

24 *L. castaneus* is a promising model to study the molecular basis of MTE tolerance.

25 **Graphical abstract**

26

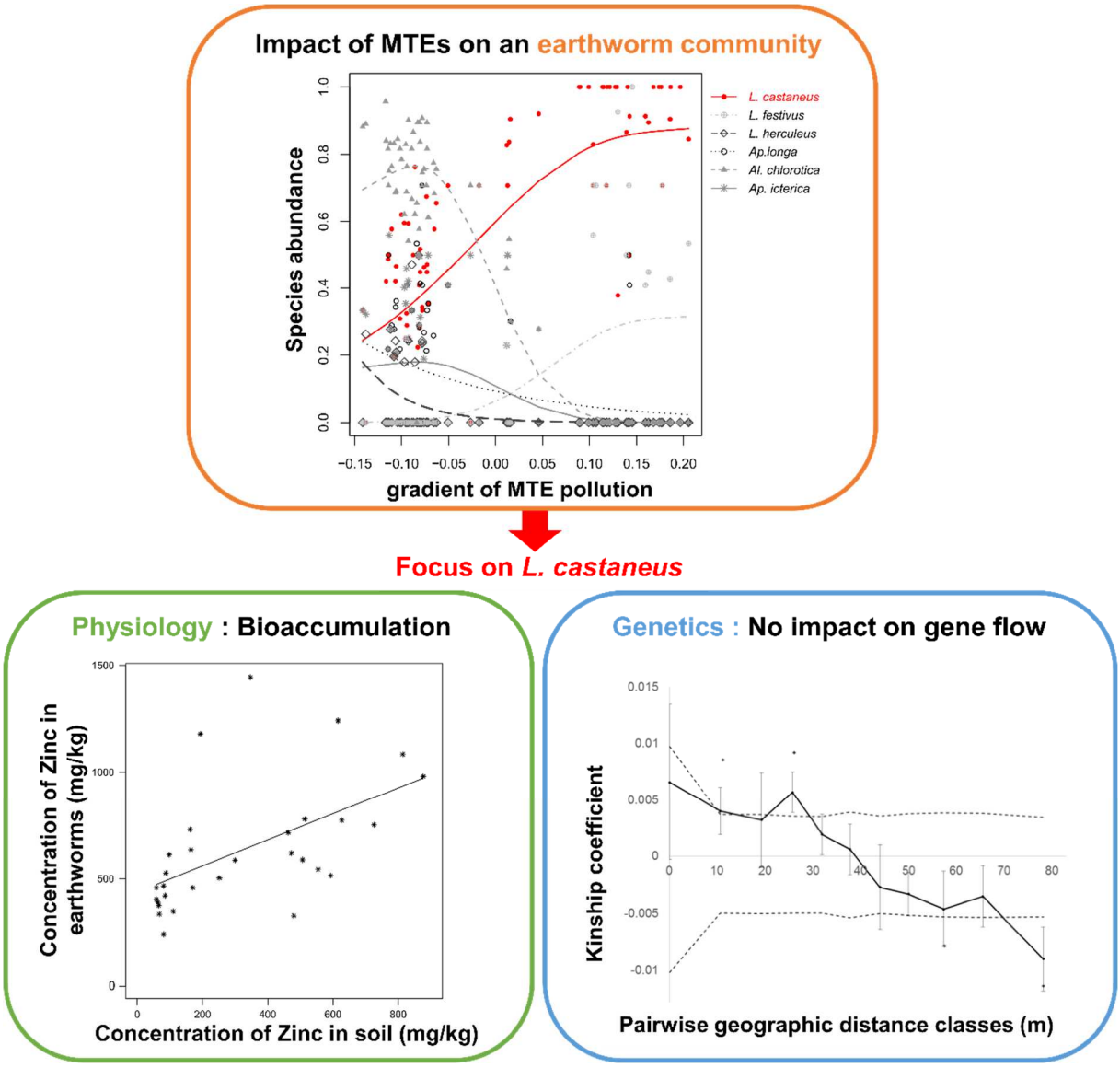

27

Abstract

Metallic trace elements (MTEs) soil pollution has become a worldwide concern, particularly regarding its impact on earthworms. Earthworms, which constitute the dominant taxon of soil macrofauna in temperate regions and are crucial ecosystem engineers, are in direct contact with MTEs. The impacts of MTE exposure on earthworms, however, vary by species, with some able to cope with high levels of contamination. We combined different approaches to study the effects of MTEs at different levels of biological organisation of an earthworm community, in a contaminated urban wasteland. Our work is based on field collection of soil and earthworm samples, with a total of 891 adult earthworms from 8 species collected, over 87 quadrats across the study plot. We found that MTE concentrations are highly structured at the plot scale and that some elements, such as Pb, Zn, and Cu, are highly correlated. Comparing species assemblage to MTE concentrations, we found that the juvenile and adult abundances, and community composition, were significantly affected by pollution. Along the pollution gradient, as species richness decreased, *Lumbricus castaneus* became more dominant. We thus investigated the physiological response of this species to a set of specific elements (Pb, Zn, Cu, and Cd) and studied the impacts of MTE concentrations at the plot scale on its population genetic. These analyses revealed that *L. castaneus* is able to bioaccumulate high quantities of Cd and Zn, but not of Cu and Pb. The population genetic analysis, based on the genotyping of 175 individuals using 8 microsatellite markers, provided no evidence of the role of the heterogeneity in MTE concentrations as a barrier to gene flow. The multidisciplinary approach we used enabled us to reveal the comparatively high tolerance of *L. castaneus* to MTE concentrations, suggesting that this is a promising model to study the molecular bases of MTE tolerance.

51 **Keywords**

52 Soil contamination, MTEs, community structure, population genetics.

53 ## 1. Introduction

54 Metallic trace elements (MTEs) occur naturally in the earth's crust, but increasing
55 quantities of metals are being released into the environment by human activities. Soil
56 pollution by MTEs has become a global concern (Hou et al., 2017; Weissmannova &
57 Pavlovsky 2017; Rodriguez-Eugenio et al., 2018), particularly in urban areas, as urban soil
58 appears to be more contaminated than agricultural and natural soils (Ajmone-Marsan &
59 Biasioli 2010). In urban soils, anthropogenic sources of MTEs include traffic emissions,
60 industrial discharges and municipal wastes (McLlwaine et al., 2017; Weissmannova &
61 Pavlovsky 2017; Jia et al., 2018). While the most common hazardous MTEs in soils (namely
62 arsenic As, cadmium Cd, chromium Cr, copper Cu, mercury Hg, nickel Ni, lead Pb and zinc
63 Zn) can be non-degradable, persistent, and bioaccumulate and biomagnify in food chains, the
64 specific impact and toxicity of the different MTEs are dictated by their chemical forms (Knox
65 et al., 2000; Weissmannova & Pavlovsky 2017). MTEs tend to accumulate in soil, and
66 sometimes in food webs, representing, beyond certain concentrations and durations of
67 exposure, a significant risk to the health of living organisms, including humans (Tyler et al.,
68 1989).

69 Earthworms constitute a dominant taxon of soil macrofauna, and their activities of
70 recycling organic matter and modifying soil structure are crucial to the functioning of the soil
71 ecosystem (Blouin et al., 2013). These keystone species are affected by MTEs present in the
72 soil as they are in direct contact with the bioavailable contaminants through the soil porewater
73 (van Gestel et al., 2009). At the community level, fieldworks showed that earthworm biomass
74 and species richness are inversely correlated to metal concentrations in the soils, and
75 especially to Pb, Zn, and Cd, contents (Terhivuo et al., 1994; Spurgeon & Hopkin 1996, 1999;
76 Nahmani et al., 2003; Leveque et al., 2015; Wang et al., 2018b). At the species level, studies
77 have aimed at evaluating metal toxicity, either focusing on their effect on fitness or assessing

78 MTE lethal and sub lethal concentrations (reviewed in Nahmani et al., 2007). However, there
79 are great differences among species in their sensitivity to MTEs. Some species of earthworms,
80 such as *Lumbricus rubellus*, *L. castaneus*, and *L. terrestris*, were shown to persist even in
81 highly contaminated sites (Spurgeon & Hopkin 1996) and this persistence can often be linked
82 with differences in physiological abilities. For instance, these species have the ability to
83 protect themselves from the toxic effects of metals by sequestering, detoxifying, and storing
84 excess metal (Spurgeon & Hopkin 1996; Vijver et al., 2004; Iordache & Borza 2012;
85 Grumiaux et al., 2015). This protection involves the induction of a gene coding a metal
86 sequestering metallothionein (Sturzenbaum et al., 1998; Brulle et al., 2006), allowing species
87 to tolerate high concentration of MTEs through bioaccumulation processes. In particular,
88 cadmium and zinc are MTEs that have been shown to bioaccumulate in numerous earthworms
89 (van Straalen et al., 2001; Tischer 2009), among which *L. castaneus* (Tischer 2009). *L.*
90 *castaneus* also accumulated higher quantities of Pb and at higher pace than *L. rubellus*,
91 *Aporrectodea caliginosa* and *A. rosea,* in a laboratory rearing experiment (Terhivuo et al.,
92 1994).

93 At the population level, MTEs are likely to induce microevolutionary processes
94 through (i) mutations and increased allelic diversity, (ii) emphasis of the effects of genetic
95 drift and bottlenecks and (iii) natural selection, leading to the disappearance of the most
96 sensitive genotypes (Ribeiro & Lopes 2013). In that respect, population genetic approaches
97 using neutral molecular markers ('neutral' refers to a locus that has no effect on fitness,
98 Holderegger et al., 2006) are commonly used to infer microevolutionary processes such as
99 mutation, genetic drift and gene flow (Kirk & Freeland 2011).

100 Since the responses of individual species and communities are highly dependent on the
101 soil physicochemical properties and the MTE cocktail present locally, the results found in the
102 literature are not always consistent (see the contrasted responses of earthworm communities

to Pb concentration from van Gestel et al., 2009 and Leveque et al., 2015). Here, we aimed at providing a comprehensive study of the effects of MTEs on different levels of the biological organisation of a community of earthworm species in a polluted site. Our approach was first exploratory and aimed at studying in their entirety the links between the concentrations of MTEs found on the study site and the earthworm community (abundance and richness). Second, we focused on the specific effect of Pb, Zn, Cd, and Cu, on *L. castaneus.* Pb, Zn, Cd, and Cu, are known to be the most widespread anthropogenic contaminant elements in urban soils (Argyraki et al., 2018), with Pb being one of the major concern in many cities (Ajmone-Marsan and Biasioli 2010). The species, *L. castaneus,* was selected as it was found throughout the site, which makes it possible to study variations in the response of this species to a range of MTE concentrations. Specifically, we hypothesized that *L. castaneus* would show increased levels of bioaccumulation with increased concentrations of these MTEs. We also investigated the neutral genetic variation of this species using 8 microsatellite markers in order to determine how mutation, genetic drift, and gene flow, affect the genetic characteristics of earthworm populations in a contaminated urban soil. To our knowledge, this is the first field study that combines different approaches to assess the responses of earthworms to metallic trace elements in the field.

2. Material and methods

2.1 Study area

The study was carried out in an urban wasteland of 8 ha situated east of the city of Villeneuve-Le-Roi, in the region of Paris (2°26'16.7"E 48°44'26.8"N, France). The area is located inside a loop of the Seine River and near an industrial zone. In 2013, a quantitative evaluation of sanitary risks was carried out at the request of the city, which wanted to convert the site and dedicate it to urban agriculture. The report concluded that an area of 3 ha north of the site presented high levels of 5 MTEs (Cd, Cu, Hg, Pb, and Zn); this polluted zone was then separated from the unpolluted zone by a fence (Guittard 2013). Further, the agro-pedological report by Sol Paysage (2013) defined the soil from the polluted zone as mainly composed of coarse sand with a C/N ratio of 14.5, a cation exchange capacity (CEC, 0-25 cm depth) of 18.7 meq/100g, and a pH of 8.2. The soil from the unpolluted zone is defined as loamy with a C/N ratio of 9.6, a CEC (0-25 cm depth) of 10.1 meq/100g, and a pH of 7.7 (Sol Paysage 2013).

The study plot covered a surface of 50 m x 60 m that straddles in approximately equal proportions the zones initially identified as polluted and unpolluted. Based on previous work on related species, this surface area is appropriate to study the fine-scale population genetic structure of earthworms in order to infer microevolutionary processes at the intra-population scale (Novo et al., 2010; Dupont et al., 2015).

2.2 Earthworms collection

Earthworms were collected over two years. The first sampling aimed to collect specimens for the studies of community structure and population genetics. It was done over three consecutive days in 2016 (March 29th, 30th, and April 1st). Earthworms were collected

from 87 quadrats (50 cm x 50 cm), chosen following a stratified sampling protocol across the study plot (Fig. 1a). 52 quadrats were sampled in the polluted zone and 35 in the unpolluted zone. We sampled more densely in the polluted zone, in order to better capture the variations in soil pollution, than in the unpolluted zone, where the soil is assumed to be homogeneous. Note that the resolution of our sampling is likely to have captured the heterogeneity of soil pollution, which is at a smaller spatial scale than the 50 cm x 50 cm quadrat of our sampling.

Over each quadrat, 10L of AITC (allyl isothyocyanate) and isopropanol diluted in water (1:100:10000L) were poured in two stages. All earthworms were collected as they came out of the soil until no more individuals came out (we waited up to 15 minutes for each quadrat). They were first transferred to a solution of 10% dilution alcohol and water, and then stored in 100% alcohol before taxonomic identification in the laboratory and analyses. The number of adults of each species as well as the number of juveniles were counted per quadrat. Earthworms were identified using the taxonomic keys of Bouché (1972) and Sims and Gerard (1999). Further, the identification of a subset of 55 individuals, for which either the taxonomic identification was uncertain or belonging to species rarely occurring within our sampling, was confronted with the results of the barcode identification, carried out using a fragment the cytochrome c oxidase subunit I (COI) mitochondrial gene (Genbank accession number MN519732 - MN519786, Hebert et al., 2003; Dupont et al., 2019).

For the second sampling, carried out the 6th of April 2017, only individuals from *L. castaneus* were collected in order to study, in this species, the bioaccumulation of a subset of MTEs. 136 *L. castaneus* individuals were sampled from 30 out of the 87 quadrats. These quadrats were selected to reflect a lead (Pb) concentration gradient (estimated on the basis of 2016 soil data, Fig. 1a).

166 **2.3 Soil collection and measure of MTE pollution**

167 Soil samples were taken simultaneously with the first earthworm sampling (in 2016) to
168 measure pH and metal pollution of soils. For each quadrat, three soil samples were collected
169 on three of the four sides of the quadrat, and pooled prior to be analyzed. In the laboratory,
170 soil samples were dried at 40°C for 24 hours, grounded, and sieved to 2 mm. Soil pH was
171 measured in 1 M KCl and in distilled H_2O according to the ISO 10390:2004 standard. The
172 concentrations of the different elements in the soils, including the MTEs, were measured by
173 X-ray Fluorescence (XRF) using the Epsilon 3XL panalytical and were analyzed with the
174 software Omnian. As soil moisture is known to significantly affect XRF-measurements
175 (Parsons et al., 2013), 10 randomly chosen soil subsamples were dried for 24 hours at 104°C
176 in order to measure their total humidity. The average soil moisture of these 10 soils was of 1.4
177 ± 0.5% (mean ± sd), which testify of the accuracy of XRF-measurements (Parsons et al.,
178 2013). However, a pilot investigation on a subset of 10 soil samples showed relatively high
179 variance of the concentrations of the different elements between 3 repeated measurements of
180 each soil sample. Therefore, for the rest of the soil samples, the measurements were
181 performed twice per sample in order to increase the reliability of measured concentrations.
182 The average concentration of each element was used in the analyses described below.
183 Detailed data on the pH and the concentrations of each element, and their variation across the
184 soil samples, are available in Table A1.

185 The variation in soil chemical composition was first explored using a PCA on zero-
186 centred and normed data of pH and concentrations of the different elements. We only
187 included in the PCA analysis the elements that were detected in a minimum of 80 quadrats.
188 The missing values were replaced by the average concentration of the element on all the
189 quadrats, so as not to influence the centroid of the PCA. Then, we tested for each element
190 their spatial autocorrelation at the scale of the sampling with a Mantel test based on 9999

191 permutations (Table A1). All the above-mentioned statistical analyses were done in R 3.6.1
192 (R core Team 2019) using the ade4 library (Dray & Dray & Dufour 2007).

193 In order to investigate bioaccumulation processes in Cd, Pb, Zn, and Cu, in *L.*
194 *castaneus* (see below), the composition of the soil samples of the 30 quadrats where *L.*
195 *castaneus* were collected for the bioaccumulation study was also quantified using inductively
196 coupled plasma-optical emission spectrometry (ICP-OES). Soil samples were first lyophilized
197 and grinded with a mortar and a pestle. The mineralisation consisted in the digestion of 300
198 mg of sample in 7 mL of concentrated HNO3, using a Berghof microwave digestion system
199 (speed wave MWS-2-Microwave pressure digestion). The soil samples were analyzed by ICP-
200 OES (ICPOES IRIS Interpid II XSP Thermo, Thermo Scientific, Whatman, MA, USA). We
201 used commercial mussel tissue (ERM®-CE278) as the certified reference material, here and
202 in the bioaccumulation study in *L. castaneus* described below. Measured concentrations in the
203 reference material never differed by more 10% from the certified concentrations.

204 **2.4 Earthworm community and soil pollution**

205 The link between earthworm assemblage and the changes in the set of chemical
206 elements detected in a minimum of 80 quadrats was performed using a canonical redundancy
207 analysis (RDA) with the Vegan package (Oksanen et al., 2018). We followed the
208 recommendation of Legendre and Gallagher (2001) and Hellinger–transformed the species
209 data prior to analysis to tune down dominant species. The statistical significance of the RDA,
210 the canonical axes, and the different elements were tested by the mean of permutation tests (n
211 = 999 permutations). For the species whose abundances showed to be significantly structured
212 by the first axis of the RDA, the shapes of these relationships were investigated. In order to
213 model changes in Hellinger-transformed abundances of species along RDA1, we used

214 generalized additive models with a quasi-Poisson family and specified the number of knots to
215 3.

216 Moreover, MTEs do not only affect adult earthworm populations. MTEs are also
217 known to interfere with species reproduction and, thereby, influence the population dynamics
218 of these species. The effects on the abundance of juveniles of the soil score on the axes of the
219 PCA (PCA1 and PCA2), while correcting for the effect of the abundance of adults present in
220 each quadrat, were tested using a generalized linear model with a Poisson distribution.

221 **2.5 Bioaccumulation of metals in whole *L. castaneus* bodies**

222 The level of MTEs in *L. castaneus* specimens were measured on individuals that were
223 starved for 48 hours to empty the intestinal content, frozen for at least 48 hours, and finally
224 lyophilized for about 60 hours. Then, the specimens were reduced to powder using liquid
225 nitrogen before mineralisation. The mineralisation is a digestion in acid medium (using
226 HNO_3, H_2SO_4 and HCl) at high temperature (for details on the method, see Bernard et al.,
227 2010). The obtained solution was analyzed by ICP-OES (Varian 720-ES, USA) and Cd, Cu,
228 Pb, and Zn, were quantified in the samples. Bioaccumulation factors (BAFs) were calculated
229 according to the following equation: $BAF_{Me} = \frac{c_{Me\ earthworm}}{c_{Me\ soil}}$, where $c_{Me\ earthworm}$ is the total
230 metal concentration in the body of the earthworm ($mg.kg^{-1}$) and $c_{Me\ soil}$ is the total
231 concentration of the same metal in the soil ($mg.kg^{-1}$). Based on preliminary visual
232 investigations of the data, the relationships between the concentration of Cd, Cu, Pb, and Zn,
233 in the specimens and in the soil were investigated using a linear model for Zn and Cd, and
234 included a quadratic term for Pb and Cu.

235 **2.6 Analysis of neutral genetic variation: microsatellite genotyping**

236 Neutral fine-scale genetic structure of *L. castaneus* populations was investigated to
237 determine if the population in the contaminated zone has undergone a strong demographic
238 bottleneck that might be linked to high mortality and to investigate if there was any limits to
239 gene flow between both plots. Total genomic DNA of 175 *L. castaneus* sampled across 63 of
240 the 87 study quadrats (Fig. 1a) was extracted using the NucleoSpin® 96 Tissue kit
241 (Macherey-Nagel). Individuals were genotyped at the eight microsatellite loci described in
242 Dupont et al. (2019). Loci were amplified by polymerase chain reaction (PCR) following the
243 protocol detailed in Dupont et al. (2019). The migration of PCR products was carried out on
244 an ABI 3130 xl Genetic Analyzer using the LIZ500 size standard (Applied Biosystems);
245 alleles were scored using GeneMapper 5 software (Applied Biosystems). All PCR results
246 were repeated and individuals missing three or more loci (e.g. failed PCR, poor-quality DNA
247 extract) were excluded from our data set.

248 The genetic diversity of the *L. castaneus* population was analyzed by computing allele
249 frequencies, number of alleles (N_{all}), and expected heterozygosity (H_e) using Genetix V 4.05
250 (Belkhir et al., 2004). The null independence between loci was tested from statistical
251 genotypic disequilibrium analysis using Genepop V4.4 (Rousset 2008). Null allele
252 frequencies were estimated using the software Microchecker (Van Oosterhout et al., 2004;
253 van Oosterhout et al., 2006). Departure from Hardy-Weinberg expectation was quantified by
254 calculating the Weir and Cockerham's (1984) estimator of the fixation index, F_{is}, and
255 conformity to Hardy-Weinberg equilibrium was assessed with exact tests implemented in
256 Genepop V4.4.

257 Moreover, we investigated the occurrence of a cryptic population structure using the
258 Bayesian model implemented in Geneland V 4.0.3 (Guillot et al., 2005) that simultaneously
259 analyses the spatial and genetic data. The analyses were conducted using both the

260 uncorrelated and correlated allele frequency models. The correlated frequency model is more
261 powerful at detecting subtle differentiation, but it is also more sensitive to departures from
262 model assumptions (e.g. presence of isolation-by-distance), and more prone to algorithm
263 instabilities, than the uncorrelated frequency model (Guillot et al., 2005). The putative
264 presence of null allele(s) was taken into account in the model (Guillot et al., 2005). The
265 Markov Chain Monte Carlo (MCMC) was run 5 times to check for convergence allowing K to
266 vary from one to three clusters and using 10^6 MCMC iterations.

267 To further examine the spatial genetic structure of *L. castaneus* at the individual scale,
268 a spatial autocorrelation analysis was conducted using Spagedi 1.2 (Hardy & Vekemans 1999;
269 Hardy & Vekemans 2002). Such an analysis provides a measure of the genetic relatedness
270 between pairs of individuals as a function of their Euclidean distances. Kinship coefficients
271 between individuals (F_{ij}) were estimated as described in Loiselle et al. (1995). We identified
272 10 classes of spatial distance in order to reach approximately 1400 pairs of individuals per
273 spatial distance class, apart from the 0 distance class with 301 pairs of individuals coming
274 from the same quadrat and having the same spatial coordinates. The average multilocus
275 relationship coefficients per distance class were estimated and their significance per class was
276 tested with 10000 permutations of multilocus genotypes. To visualize the spatial genetic
277 structure, we plotted the kinship coefficient against geographical distance.

278 **3. Results**

279 **3.1 Soil pollution heterogeneity**

280 XRF-measurements allowed the relative quantification of 38 elements over all soils
281 sampled. First, it was shown that the concentrations of elements greatly varied among
282 samples. Al, As, Ca, Cr, Fe, K, Mg, Mn, Pb, Rb, S, Si, Sr, Ti, V, Zn, Zr were found in each of

the 87 soils sampled (Table A1). Ba, Eu, Ga, Hg, Ir, Mo, Nb, Ni, Os, Re, Sb, Ta, Te, Th, Yb were found in less than 64 of the sampled soils (Table A1). The accuracy of the XRF-measurements greatly varied between measurements and between elements. For example, the coefficient of variation between replicate measurements for As, S, and Cr were of 52.5, 26.1, and 15.8%, respectively. Therefore, even though these elements were also found to significantly vary among samples, suggesting that they are likely to structure the environment, their potential effect should be interpreted with caution as the reliability of their quantification is uncertain. However, for Pb, Cu, and Zn, which are the MTEs of interest, the coefficients of variation among XRF-measures were quite low (from 6.5 to 11.2, Table A1). The XRF-measures for these elements were also highly correlated with the measurements obtained by ICP-OES (Pb: $r = 95.3$, $n = 30$, $p < 0.001$; Cu: $r = 78.0$, $n = 28$, $p < 0.001$; Zn: $r = 99.4$, $n = 30$, $p < 0.001$), suggesting that their quantification by XRF is reliable. Cd, which is also a MTE of interest, was always below the level of detection by XRF.

The two first axes of the PCA capture 66.6% of the variation in chemical composition found between soil samples (Fig. 1b). The first axis accounts for most of the variation, 52.9%, found among soil samples. This axis is characterized by soils mainly rich in Ti, K, Al, Rb, and Si, at one end, and in Sr, Pb, Zn, Ca, and Cu, at the other end. Soil contamination in Pb, Zn, and Cu, is highly correlated (Fig. 1b). Besides, Mantel's tests have shown that most of the elements that contribute the most to PCA1 also exhibit strong spatial autocorrelation, as is the case for Pb, Zn, and Cu (Mantel test: Pb = 0.44, $p < 0.001$; Zn = 0.40, $p < 0.001$; Cu = 0.25, $p < 0.001$, see Table A1). Such a spatial autocorrelation suggests that the pollution is structured at the scale of our sampling. The visual inspection of the interpolation plot for PCA1 shows that the pollution is indeed structured with a source pollution at the northwest of the site (Fig. 1a, Appendix B).

307 **3.2 Community composition**

308 A total of 891 adults, 21 subadults, and 1129 juveniles, were collected over the 87
309 samples. On average, we found 10.24 ± 0.92 adults, 12.98 ± 1.33 juveniles, and a juvenile to
310 adult ratio of 1.54 ± 0.15 in each quadrat (mean ± se). No earthworm was collected in four out
311 of the 87 quadrats. Eight species were found: *Al. chlorotica* (L1, n = 418), *L. castaneus* (n =
312 279), *Ap. rosea* (L4, n = 49), *Ap. icterica* (n = 47), *Ap. longa* (n = 38), *L. festivus* (n = 25), *Ap.*
313 *giardi* (n = 15), *L. herculeus* (n = 14). We were also able to identify subadults of *Ap. longa* (n
314 = 7), *L. festivus* (n = 6), *Ap. giardi* (n = 4), *Al. chlorotica* (L1, n = 2), and of *Ap. rosea* (L4, n
315 = 2).

316 The canonical RDA showed that soil chemical composition accounted for 43.1% of
317 the variation in species abundance and the permutation test confirmed the significance of this
318 model (F = 3.88, p = 0.001, Fig. 2a). Only the first axis of the RDA (RDA1) was significant
319 (F = 81.84, p = 0.001) and explained 35.4% of the total variance. pH H_2O, Mg, and Fe,
320 significantly explained the variation captured by the RDA (F(pH H_2O) = 32.75, p = 0.001;
321 F(Mg) = 26.73, p = 0.001; F(Fe) = 4.09, p = 0.009). Although not found to be significant, the
322 first axis aligns closely with an increase in the concentration of soils in Cu, Zn, and Pb (Fig.
323 2a). Thus, in what follows, we interpret the changes in community composition along the first
324 axis of the RDA as a response to an increase of MTE pollution.

325 The generalized additive models built to investigate for each species changes in the
326 Hellinger-transformed abundance data along RDA1 were significant for 6 of the 8 recorded
327 species and highlighted species differences of sensitivity to soil pollution by MTEs (Fig. 2b,
328 Table A2). Note that while the models were not significant for *Ap. rosea* and *Ap. giardi,* these
329 species were not observed in soils with high scores on the RDA1. Still, in the following our
330 interpretations are limited to the changes in these 6 species, which significantly vary along
331 RDA1. For high RDA1 values, species richness is restricted to *L. festivus* and *L. castaneus*,

332 the latter being the dominant species. For low RDA1 values, the communities are much more
333 diverse, with the all 6 species being observed in soils with low scores on RDA1. The relative
334 dominance of *Al. chlorotica* in the community sharply decreased with increasing values along
335 the RDA1 axis, as for *Ap. icterica, Ap. longa,* and *L. herculeus,* but the amplitudes of their
336 variation were weaker (Fig. 2b). *L. festivus* was not observed for soils with a low score on
337 RDA1. The explained deviations of the models were high, up to 90.3% for *Al. chlorotica,*
338 suggesting that changes in species abundance and of community assemblage is to a large
339 extent determined by changes in soil chemical composition (Table A2). More specifically,
340 these changes in species abundance along RDA1 are likely to reflect, in part, the increase in
341 concentrations of MTEs in soils, and in particular of Zn, Pb, and Cu (Fig. 2a).

342 Last, the number of juveniles is positively correlated to the number of adults (estimate
343 = 0.051, z-value = 16.74, $p < 0.001$, Table A3). In addition, the number of juveniles is
344 negatively correlated to PCA1 (estimate = -0.090, z-value = -6.57, $p<0.001$) but positively
345 correlated to PCA2 (estimate = 0.13, z-value = 6.47, $p<0.001$).

346 **3.3 Bioaccumulation in *L. castaneus***

347 *L. castaneus* showed high BAFs for Zn [0.68 – 7.81] and Cd [5.41 – 56.97]. The
348 models testing the relationship between the concentration of MTEs in earthworms and the
349 soils showed that bioaccumulation of Zn and Cd by *L. castaneus* was linear (Fig. 3). The
350 models explained 25.9 and 22.3 % of the variance in the data for Zn and Cd, respectively. In
351 contrast, *L. castaneus* showed low BAFs for Cu [0.0027 – 0.26] and Pb [0.005 – 0.23],
352 indicating that at the site, these MTEs do not bioaccumulate in *L. castaneus*. Yet, the
353 concentrations of Cu and Pb in earthworms and the soils are correlated according to a
354 quadratic relationship. The models captured 33.5% and 39.7% of the variance in the data for
355 Cu and Pb, respectively (Fig. 3).

356 **3.4 Population genetic structure of *L. castaneus***

357 A high neutral genetic diversity was observed within the 175 analysed genotypes (N_{all}
358 = 16.25; H_e = 0.670). Two pairs of loci departed significantly from linkage equilibrium (LC18
359 – LC33 and LC10-LC36). Since Dupont et al. (2019) showed no physical linkage between
360 these loci, this result could be explained by inbreeding (Nordborg 2000). A second dataset
361 composed of only one genotype per quadrat (i.e. 63 genotypes) was created. All loci were
362 unlinked in this second dataset and a lower proportion of them displayed heterozygote
363 deficiency (i.e. significant F_{is} estimate, Table 1). Geneland Bayesian analysis requiring
364 linkage equilibrium was carried out with this second dataset and identified only one group of
365 individuals in the study plot, regardless of the model of allelic frequency chosen.

366 Spatial autocorrelation analysis revealed, however, local genetic structure at the scale
367 of the study plot. We found a significant negative relationship between the kinship coefficient
368 and the geographic distance between pair of individuals (b ± se = -0.211 ± 0.079, $p < 0.001$).
369 In particular, positive values of kinship coefficient are measured between individuals
370 collected in close quadrats (mean distance of 10 m and 25 m), which means that neighbouring
371 individuals have a higher genetic relatedness than random pairs of individuals (Fig. 4).
372 Conversely, negative kinship coefficient values, are observed between individuals collected in
373 more distant quadrats (mean distance of 60m and 80m) and indicate isolation by distance (Fig.
374 4).

375 **4. Discussion**

376 The study plot displays a high heterogeneity in soil chemical composition. In
377 particular, the concentrations of MTEs are highly structured and reflect the division of the plot
378 into the polluted and unpolluted zones. The levels of pollution in Pb, Cu, Cd, and Zn, overlap

379 with the range of variation found elsewhere in lawn and forest soils of the Paris region (Foti et
380 al., 2017) and the median value of European urban soils and world soils for Pb, Cu, Zn, Ni,
381 Cr, Cd, and As (Baize 1997; Adriano 2001; Desaules 2012; Luo et al., 2012, summarized in
382 Foti et al., 2017). The concentrations of MTEs were, for part, highly correlated, which makes
383 it difficult to disentangle their respective impact on earthworms, suggesting potential cocktail
384 effects. Based on the existing knowledge and literature on the impact of MTEs on earthworm
385 species, in the following we relate the variation of soil chemical composition along RDA1 to
386 a gradient of pollution, since this axis is associated with increasing concentrations of Pb, Cu,
387 and Zn (Fig. 2a).

388 **4.1 Impact of MTEs on earthworm community**

389 Along the gradient of pollution, we observed marked changes in community
390 composition and abundances. *Al. chlorotica* and *L. castaneus* were the dominant species in
391 our sampling. *Al. chlorotica* dominates low-polluted quadrats and is absent from the most
392 polluted part of the plot, while the relative abundance of *L. castaneus* increases along the
393 pollution gradient. Previous studies have already shown that epigeic species, such as *L.*
394 *castaneus*, are more resistant than endogeic species, such as *Al. chlorotica*, to the effects of
395 MTE pollution (e.g. Spurgeon & Hopkin 1999; Mirmonsef et al., 2017). An explanation for
396 this difference is that endogeic species that live and feed in the mineral soil layers are
397 probably more exposed to the bioavailable fraction of metals, per comparison with epigeic
398 species which are active in the superficial soil and litter layers (Mirmonsef et al., 2017).
399 Overall, species richness decreased along the pollution gradient, as did the abundance
400 of juveniles compared to that of adults. The latter result is consistent with the literature as Cd,
401 Pb, Cu, and Zn, are known to reduce reproduction rates in several species. For instance,
402 Spurgeon et al. (1994) found a significant negative effect of high concentrations of these four

403 MTEs, particularly of Cd and Cu, on the cocoon production of the epigeic earthworm *Eisenia*
404 *fetida* in an artificial soil. Significant decreases in cocoon production was also observed for *L.*
405 *rubellus* in Cu-amended sandy soil and sandy loam (Ma 1984). Conversely, Reinecke et al.
406 (2001) showed that in three different species, *Eudrilus eugeniae*, *Perionyx excavates*, and *E.*
407 *fetida*, cocoon viability, but not production, was detrimentally affected by Pb concentrations.

408 Although MTEs are known to have an impact on earthworms, we cannot exclude the
409 hypothesis that the observed changes of community composition across the plot may be
410 explained by differences in soil properties between zones. The unpolluted zone is
411 characterized by a sandy soil while a loamy soil was found in the polluted zone, and these
412 differences also have certainly an impact on the earthworm community composition. Indeed,
413 spatial variations in the abundance of earthworms are commonly observed and can be partly
414 explained by variations in soil properties (e.g. Nuutinen et al., 1998). It is however
415 noteworthy that the most abundant earthworm species in the polluted zone is *L. castaneus*, an
416 epigeic species known to resist to and bioaccumulate MTEs (present study, Terhivuo et al.,
417 1994; Spurgeon & Hopkin 1996; Tischer 2009).

418 **4.2 Impact of MTEs on the bioaccumulation of *L. castaneus***

419 We showed that *L. castaneus* bioaccumulate Zn and Cd, and that the bioaccumulation
420 of these two MTEs was highly correlated ($R^2 = 0.89$, $t = 10.5$, $p < 0.001$).

421 Zn is an essential element necessary for earthworm growth, maturation, and
422 reproduction, and might therefore be required to a number of metabolic processes (Nannoni et
423 al., 2014; Wang et al., 2018a). High concentrations of Zn in earthworm tissues have been
424 recorded elsewhere (Wang et al., 2018a) but it has also been shown that some earthworm
425 species, e.g. *Eisenia fetida*, are able to regulate their uptake of Zn and, thus, do not
426 accumulate this metal (Bernard et al., 2010; Brulle et al., 2011). In our sampling, *L. castaneus*

427 was found to accumulate Zn up to 7.8 fold the concentration found in the soil. The
428 relationship between the concentration of Zn in *L. castaneus* and in soil is linear, suggesting
429 that the bioaccumulation of Zn has not reached a threshold.

430 Although the concentration of Cd was relatively low in the soil, ranging from 0.15 to
431 1.06 mg/kg, this metal accumulated in *L. castaneus* up to 18.06 mg/kg, a result highlighting
432 its strong bioavailability. *L. castaneus* wasshown to bioaccumulate up to 56.9 fold the
433 concentration of Cd found in the surrounding soil. This strong ability to accumulate Cd has
434 been reported for other epigeic and endogeic earthworm species (Bernard et al., 2010; Latif et
435 al., 2013).

436 Conversely, the bioaccumulation factors of Pb and Cu in *L. castaneus* were low. Other
437 studies have shown that Cu and Pb are bioaccumulated by earthworms when their
438 concentrations in soils are particularly high ([Pb] > 900 mg/kg Bernard et al., 2010). The soil
439 concentrations of Cu and Pb at our study site are, comparatively, lower, which might explain
440 why these metals were not found to bioaccumulate in *L. castaneus.* Alternatively, Mirmonsef
441 et al. (2017) proposed that the bioaccumulation of Cu or other heavy metals in earthworm
442 populations can occur in populations that have been exposed for many generations to these
443 metals, as natural selection and genetic adaptation in these populations would have resulted in
444 an increase in their efficiency to sequester and detoxify these MTEs. The low
445 bioaccumulation of Cu and Pb by the population of *L. castaneus* at our study site could then
446 reflect the yet limited duration of their exposure to pollution.

447 **4.3 Impact of MTEs on the genetic characteristics of *L. castaneus***

448 The genetic variability of a population exposed to MTEs may be altered in different
449 ways. Genetic changes in the population may either result from genotoxic exposure (i.e. direct
450 effect) or from microevolutionary processes (i.e. indirect effect). Direct effects are related to

451 DNA or chromosome alterations which, when they are exerted on gametes and are passed on
452 to the next generation, can significantly impact exposed populations (Medina et al., 2007). In
453 this work, we focused on indirect effects of MTEs, which are population-mediated processes.
454 We assumed that soil pollution by MTEs may alter the diversity of neutral genetic markers,
455 such as microsatellites, through random genetic drift associated to drastic reduction in
456 population size. However, the indices of genetic diversity computed in the population were
457 high, similar to those of other *L. castaneus* populations genotyped with the same markers
458 (Dupont et al., 2019), providing no support for the hypothesis that this population would have
459 undergone a significant reduction of genetic diversity through genetic drift. Alternatively, the
460 genetic structure estimated from neutral markers could be shaped by natural selection of
461 resistant phenotypes. In such instance, we would expect to observe at least two differentiated
462 genetic clusters, corresponding to the polluted and unpolluted zones. Yet, no genetic
463 clustering was revealed at the scale of the study plot. Last, the spatial autocorrelation analysis
464 revealed a pattern of isolation by distance that does not support the role of the heterogeneity
465 of soil pollution by MTEs as a barrier to gene flow in this species. This result, added to the
466 fact that the abundance of *L. castaneus* was found to be high in the polluted quadrats, suggest
467 that direct genotoxic effects might be negligible for this species.

468 **5. Conclusion**

469 It is particularly difficult to study the consequences of MTE pollution on soil
470 biodiversity in the field, mainly because of confounding and cocktail effects (e.g. Ye et al.,
471 2017). Although laboratory experiments are valuable in testing theory and in providing
472 quantitative estimates of survival and reproduction rates of species under controlled
473 conditions (e.g. level of contamination), they can be difficult to implement when the pollution
474 is multifactorial and heterogeneous, as generally observed in urban areas. Moreover, these

475 experiments frequently use the laboratory earthworm models, *E. fetida* and *E. andrei,* while
476 they are often rare in the field (e.g. Coelho et al., 2018).

477 Here, we used a multidisciplinary approach to study in the field the response to MTE
478 pollution of an earthworm community in an urban area and to further our understanding of the
479 bioaccumulation capacities, population genetic structure and gene expression of a MTE
480 tolerant species in response to pollution. *L. castaneus* was identified as the most tolerant
481 species to MTEs of the study site. In sites contaminated by MTEs, the maintenance of
482 earthworm populations and their associated functions in the ecosystem (Pauwels et al., 2013)
483 rely on the evolution of molecular mechanisms of metal tolerance, which, however, remain
484 poorly understood. As mentioned elsewhere (Stapley et al., 2010; Vandegehuchte & Janssen
485 2014; Evans 2015), the study of gene expression profile in populations under different
486 selection pressure should provide new insights into the molecular mechanisms of metal
487 tolerance in earthworms, and help identify candidate functional genes that may be under
488 selection. Although still expensive, the Next-generation sequencing (NGS), now permits
489 direct transcriptome sequencing, and can provide such qualitative and quantitative
490 information on the expression of genes.

Acknowledgements

This work was funded by the Ile de France region through the "Partenariats institutions-citoyens pour la recherche et l'innovation" (Picri) calls for projects (ReFUJ project). H. Audusseau acknowledges support from the Swedish Research Council (2016-06737). This work benefited from discussions with J. Mathieu (Sorbonne – University) and T. Lerch (UPEC).

References

Adriano DC (2001) Trace metals in terrestrial environments: biogeochemistry, bioavailability and risks of metals, p. 866. Springer-Verlag, New York.

Ajmone-Marsan F & Biasioli M (2010) Trace elements in soils of urban areas. Water Air and Soil Pollution, 213, 121-143.

Argyraki A, Kelepertzis E, Botsou F, Paraskevopoulou V, Katsikis I & Trigoni M (2018) Environmental availability of trace elements (Pb, Cd, Zn, Cu) in soil from urban, suburban, rural and mining areas of Attica, Hellas. Journal of Geochemical Exploration, 187, 201-213.

Baize D (1997) Teneurs totales en éléments traces métalliques dans les sols (France). Références et stratégies d'interprétation., p. 410. INRA Editions, Paris.

Belkhir K, Borsa P, Goudet J, Chikhi L & Bonhomme F (2004) GENETIX 4.05, logiciel sous Windows pour la génétique des populations. Laboratoire Génome, Population, Interactions, CNRS UMR 5000, Université Montpellier II, Montpellier (France).

Bernard F, Brulle F, Douay F, Lemiere S, Demuynck S & Vandenbulcke F (2010) Metallic trace element body burdens and gene expression analysis of biomarker candidates in *Eisenia fetida*, using an "exposure/depuration" experimental scheme with field soils. Ecotoxicology and Environmental Safety, 73, 1034-1045.

Blouin M, Hodson ME, Delgado EA, Baker G, Brussaard L, Butt KR, Dai J, Dendooven L, Peres G, Tondoh JE, Cluzeau D & Brun JJ (2013) A review of earthworm impact on soil function and ecosystem services. European Journal of Soil Science, 64, 161-182.

Bouché MB (1972) Lombriciens de France. Ecologie et systématique INRA, Paris.

Brulle F, Lemiere S, Waterlot C, Douay F & Vandenbulcke F (2011) Gene expression analysis of 4 biomarker candidates in *Eisenia fetida* exposed to an environmental metallic trace elements gradient: A microcosm study. Science of the Total Environment, 409, 5470-5482.

Brulle F, Mitta G, Cocquerelle C, Vieau D, Lemiere S, Lepretre A & vandenBulcke F (2006) Cloning and real-time PCR testing of 14 potential biomarkers in *Eisenia fetida* following cadmium exposure. Environmental Science & Technology, 40, 2844-2850.

Coelho C, Foret C, Bazin C, Leduc L, Hammada M, Inacio M & Bedell JP (2018) Bioavailability and bioaccumulation of heavy metals of several soils and sediments (from industrialized urban areas) for *Eisenia fetida*. Science of the Total Environment, 635, 1317-1330.

Desaules A (2012) Critical evaluation of soil contamination assessment methods for trace metals. Science of the Total Environment, 426, 120-131.

Dray S & Dufour AB (2007) The ade4 package: implementing the duality diagram for ecologists. Journal of Statistical Software, 22, 1-20.

Dupont L, Grésille Y, Richard B, Decaëns T & Mathieu J (2015) Fine-scale spatial genetic structure and dispersal constraints in two earthworm species. Biological Journal of the Linnean Society, 114, 335-347.

Dupont L, Pauwels M, Dume C, Deschins V, Audusseau H, Gigon A, Dubs F & Vandenbulcke F (2019) Genetic variation of the epigeic earthworm *Lumbricus*

castaneus populations in urban soils of the Paris region (France) revealed using eight newly developed microsatellite markers. Applied Soil Ecology, 135, 33-37.

Evans TG (2015) Considerations for the use of transcriptomics in identifying the 'genes that matter' for environmental adaptation. Journal of Experimental Biology, 218, 1925-1935.

Foti L, Dubs F, Gignoux J, Lata J-C, Lerch TZ, Mathieu J, Nold F, Nunan N, Raynaud X, Abbadie L & Barot S (2017) Trace element concentrations along a gradient of urban pressure in forest and lawn soils of the Paris region (France). Science of the Total Environment, 598, 938-948.

Grumiaux F, Demuynck S, Pernin C & Lepretre A (2015) Earthworm populations of highly metal-contaminated soils restored by fly ash-aided phytostabilisation. Ecotoxicology and Environmental Safety, 113, 183-190.

Guillot G, Mortier F & Estoup A (2005) Geneland : A program for landscape genetics. Molecular Ecology Notes, 5, 712-715.

Guittard A (2013) Evaluation quantitative des risques sanitaires (EQRS) du site de Pierre Frite à Villeneuve-Le-Roi (94) (ed. CG94). BG Ingénieurs Conseils.

Hardy OJ & Vekemans X (1999) Isolation by distance in a continuous population: reconciliation between spatial autocorrelation analysis and population genetics models. Heredity, 83, 145-154.

Hardy OJ & Vekemans X (2002) SPAGEDi: a versatile computer program to analyse spatial genetic structure at the individual or population levels. Molecular Ecology Notes, 2, 618-620.

Hebert PDN, Cywinska A, Ball SL & Dewaard JR (2003) Biological identifications through DNA barcodes. Proceedings of the Royal Society of London Series B: Biological Sciences, 270, 313-321.

Holderegger R, Kamm U & Gugerli F (2006) Adaptive vs. neutral genetic diversity: implications for landscape genetics. Landscape Ecology, 21, 797-807.

Hou DY, O'Connor D, Nathanail P, Tian L & Ma Y (2017) Integrated GIS and multivariate statistical analysis for regional scale assessment of heavy metal soil contamination: A critical review. Environmental Pollution, 231, 1188-1200.

Iordache M & Borza I (2012) The bioremediation potential of earthworms (Oligochaeta: Lumbricidae) in a soil polluted with heavy metals. Journal of Food Agriculture & Environment, 10, 1183-1186.

Jia Z, Li S & Wang L (2018) Assessment of soil heavy metals for eco-environment and human health in a rapidly urbanization area of the upper Yangtze Basin. Scientific Reports, 8, 3256.

Kirk H & Freeland JR (2011) Applications and implications of neutral versus non-neutral markers in Molecular Ecology. International Journal of Molecular Sciences, 12, 3966-3988.

Knox A, Seamans JC, Mench MJ & Vangronseveld J (2000) Remediation of metal-and radionuclides- contaminated soils by in situ stabilization techniques. In: Environmental restoration of metals-contaminated soils (ed. Islandar, I.K.). Lewis Publishers, Boca Raton.

582 Latif R, Malek M & Mirmonsef H (2013) Cadmium and lead accumulation in three endogeic
583 earthworm species. Bulletin of Environmental Contamination and Toxicology, 90,
584 456-459.

585 Legendre P & Gallagher ED (2001) Ecologically meaningful transformations for ordination of
586 species data. Oecologia, 129, 271-280.

587 Leveque T, Capowiez Y, Schreck E, Mombo S, Mazzia C, Foucault Y & Foucault G (2015)
588 Effects of historic metal(loid) pollution on earthworm communities. Science of the
589 Total Environment, 511, 738-746.

590 Loiselle BA, Sork VL, Nason J & Graham C (1995) Spatial genetic structure of a tropical
591 understory shrub, *Psychotria officinalis* (Rubiaceae). American Journal of Botany, 82,
592 1420-1425.

593 Luo XS, Yu S, Zhu YG & Li XD (2012) Trace metal contamination in urban soils of China.
594 Science of the Total Environment, 421, 17-30.

595 Ma W (1984) Sublethal toxic effects of copper on growth, reproduction and litter breakdown
596 activity in the earthworm *Lumbricus rubellus*, with observations on the influence of
597 temperature and soil pH. . Environmental Pollution Series a-Ecological and
598 Biological, 33, 207-219.

599 McLlwaine R, Doherty R, Cox SF & Cave M (2017) The relationship between historical
600 development and potentially toxic element concentrations in urban soils.
601 Environmental Pollution, 220, 1036-1049.

602 Medina MH, Correa JA & Barata C (2007) Micro-evolution due to pollution: possible
603 consequences for ecosystem responses to toxic stress. Chemosphere, 67, 2105-2114.

604 Mirmonsef H, Hornum HD, Jensen J & Holmstrup M (2017) Effects of an aged copper
605 contamination on distribution of earthworms, reproduction and cocoon hatchability.
606 Ecotoxicology and Environmental Safety, 135, 267-275.

607 Nahmani J, Hodson ME & Black S (2007) A review of studies performed to assess metal
608 uptake by earthworms. Environmental Pollution, 145, 402-424.

609 Nahmani J, Lavelle P, Lapied E & van Oort F (2003) Effects of heavy metal soil pollution on
610 earthworm communities in the north of France. Pedobiologia, 47, 663-669.

611 Nannoni F, Rossi S & Protano G (2014) Soil properties and metal accumulation by
612 earthworms in the Siena urban area (Italy). Applied Soil Ecology, 77, 9-17.

613 Nordborg M (2000) Linkage disequilibrium, gene trees and selfing: An ancestral
614 recombination graph with partial self-fertilization. Genetics, 154, 923-929.

615 Novo M, Almodovar A, Fernandez R, Gutierrez M & Cosin DJD (2010) Mate choice of an
616 endogeic earthworm revealed by microsatellite markers. Pedobiologia, 53, 375-379.

617 Nuutinen V, Pitkanen J, Kuusela E, Widbom T & Lohilahti H (1998) Spatial variation of an
618 earthworm community related to soil properties and yield in a grass-clover field.
619 Applied Soil Ecology, 8, 85-94.

620 Oksanen J, Blanchet FG, Friendly M, Kindt R, Legendre P, McGlinn D, Minchin PR, O'Hara
621 RB, Simpson GL, Solymos P, Stevens MH, Szoecs E & Wagner HH (2018) vegan:
622 Community Ecology Package. R package version 2.5-3.

623 Parsons C, Grabulosa EM, Pili E, Floor GH, Roman-Ross G & Charlet L (2013)
624 Quantification of trace arsenic in soils by field-portable X-ray fluorescence

spectrometry: Considerations for sample preparation and measurement conditions. Journal of Hazardous Materials, 262, 1213-1222.

Pauwels M, Frerot H, Souleman D & Vandenbulcke F (2013) Using biomarkers in an evolutionary context: Lessons from the analysis of biological responses of oligochaete annelids to metal exposure. Environmental Pollution, 179, 343-350.

Reinecke AJ, Reinecke SA & Maboeta MS (2001) Cocoon production and viability as endpoints in toxicity testing of heavy metals with three earthworm species. Pedobiologia, 45, 61-68.

Ribeiro R & Lopes I (2013) Contaminant driven genetic erosion and associated hypotheses on alleles loss, reduced population growth rate and increased susceptibility to future stressors: an essay. Ecotoxicology, 22, 889-899.

Rodriguez-Eugenio N, McLaughlin M & Pennock D (2018) Soil pollution : a hidden reality, p. 142. FAO.

Rousset F (2008) GENEPOP ' 007: a complete re-implementation of the GENEPOP software for Windows and Linux. Molecular Ecology Resources, 8, 103-106.

Sims RW & Gerard BM (1999) Synopsis of the British Fauna (31)- earthworms, pp. 1-169. The Linnean Society of London and the Estuarine and Brackish-water Sciences association, London.

Snape JR, Maund SJ, Pickford DB & Hutchinson TH (2004) Ecotoxicogenomics: the challenge of integrating genomics into aquatic and terrestrial ecotoxicology. Aquatic Toxicology, 67, 143-154.

Sol Paysage (2013) Villeneuve-Le-Roi Projet d'aménagement d'une friche - Pierrefrite. Rapport d'études agro-pédologiques. Conseil Général 94, Orsay.

Spurgeon DJ & Hopkin SP (1996) The effects of metal contamination on earthworm populations around a smelting works: Quantifying species effects. Applied Soil Ecology, 4, 147-160.

Spurgeon DJ & Hopkin SP (1999) Seasonal variation in the abundance, biomass and biodiversity of earthworms in soils contaminated with metal emissions from a primary smelting works. Journal of Applied Ecology, 36, 173-183.

Spurgeon DJ, Hopkin SP & Jones DT (1994) Effects of cadmium, copper, lead and zinc on growth, reproduction and survival of the earthworm *Eisenia fetida* (Savigny) - Assessing the environmental impact of point-source metal contamination in terrestrial ecosystems. Environmental Pollution, 84, 123-130.

Stapley J, Reger J, Feulner PGD, Smadja C, Galindo J, Ekblom R, Bennison C, Ball AD, Beckerman AP & Slate J (2010) Adaptation genomics: the next generation. Trends in Ecology & Evolution, 25, 705-712.

Sturzenbaum SR, Kille P & Morgan AJ (1998) Heavy metal-induced molecular responses in the earthworm, *Lumbricus rubellus* genetic fingerprinting by directed differential display. Applied Soil Ecology, 9, 495-500.

Terhivuo J, Pankakoski E, Hyvarinen H & Koivisto I (1994) Pb uptake by ecologically dissimilar earthworm (lumbricidae) species near a lead smelter in South Finland. Environmental Pollution, 85, 87-96.

Tischer S (2009) Earthworms (Lumbricidae) as bioindicators: the relationship between in-soil and in-tissue heavy metal content. Polish Journal of Ecology, 57, 513-523.

Tyler G, Pahlsson AMB, Bengtsson G, Baath E & Tranvik L (1989) Heavy-metal ecology of terrestrial plants, microorganisms and invertebrates - a review. Water Air and Soil Pollution, 47, 189-215.

van Gestel CAM, Koolhaas JE, Hamers T, van Hoppe M, van Roovert M, Korsman C & Reineckec SA (2009) Effects of metal pollution on earthworm communities in a contaminated floodplain area: Linking biomarker, community and functional responses. Environmental Pollution, 157, 895-903.

Van Oosterhout C, Hutchinson WF, Wills DPM & Shipley P (2004) MICRO-CHECKER: software for identifying and correcting genotyping errors in microsatellite data. Molecular Ecology Notes, 4, 535-538.

van Oosterhout C, Weetman D & Hutchinson WF (2006) Estimation and adjustment of microsatellite null alleles in nonequilibrium populations. Molecular Ecology Notes, 6, 255-256.

van Straalen NM, Butovsky RO, Pokarzhevskii AD, Zaitsev AS & Verhoef SC (2001) Metal concentrations in soil and invertebrates in the vicinity of a metallurgical factory near Tula (Russia). Pedobiologia, 45, 451-466.

Vandegehuchte MB & Janssen CR (2014) Epigenetics in an ecotoxicological context. Mutation Research-Genetic Toxicology and Environmental Mutagenesis, 764, 36-45.

Vijver MG, Van Gestel CAM, Lanno RP, Van Straalen NM & Peijnenburg W (2004) Internal metal sequestration and its ecotoxicological relevance: A review. Environmental Science & Technology, 38, 4705-4712.

Wang K, Qiao Y, Zhang H, Yue S, Li H, Ji X & Liu L (2018a) Bioaccumulation of heavy metals in earthworms from field contaminated soil in a subtropical area of China. Ecotoxicology and Environmental Safety, 148, 876-883.

Wang K, Qiao YH, Zhang HQ, Yue SZ, Li HF, Ji XH & Crowley D (2018b) Influence of cadmium-contaminated soil on earthworm communities in a subtropical area of China. Applied Soil Ecology, 127, 64-73.

Weir BS & Cockerham CC (1984) Estimating F-statistics for the analysis of population structure. Evolution, 38, 1358-1370.

Weissmannova HD & Pavlovsky J (2017) Indices of soil contamination by heavy metals - methodology of calculation for pollution assessment (minireview). Environmental Monitoring and Assessment, 189, 616.

Ye SJ, Zeng GM, Wu HP, Zhang C, Liang J, Dai J, Liu ZF, Xiong WP, Wan J, Xu PA & Cheng M (2017) Co-occurrence and interactions of pollutants, and their impacts on soil remediation-A review. Critical Reviews in Environmental Science and Technology, 47, 1528-1553.

705 **Figure legends**

706 **Figure 1** (a) Interpolation maps of soil score on PCA1. We interpolated the data using
707 ordinary kriging and validated our interpolation plot by cross validation of the residuals (see
708 Appendix B for further explanation on the interpolation plot). The pie charts indicate the
709 location of the quadrats and the purpose which the collected earthworms were used for. (b)
710 Biplot showing the contribution to the two PCA axes of pH and chemical elements, as well as
711 the position of soil samples (quadrats) in this two-dimensional space.

712

713 **Figure 2** (a) RDA triplots of the Hellinger-transformed earthworm abundance data
714 constrained by the elements measured in a minimum of 80 quadrats. (b) Changes in Hellinger-
715 transformed abundance data along RDA1 for *L. castaneus, L. festivus, L. herculeus, Ap.longa,*
716 *Al. chlorotica,* and *Ap. icterica*. The fitted GAM is depicted by a line for each species and the
717 dots correspond to the raw data.

718

719 **Figure 3** Relationship between the concentrations of MTEs measured by ICP in earthworms
720 and soils for Cu and Pb (left panel), Zn (central panel), and Cd (right panel).

721

722 **Figure 4** Average kinship coefficients, F_{ij}, between pairs of *L. castaneus* individuals plotted
723 against the geographical distance. Dashed lines represent 95% confidence intervals for F_{ij}
724 under the null hypothesis that genotypes are randomly distributed. Significant values: *P <
725 0.05.

Figure 1

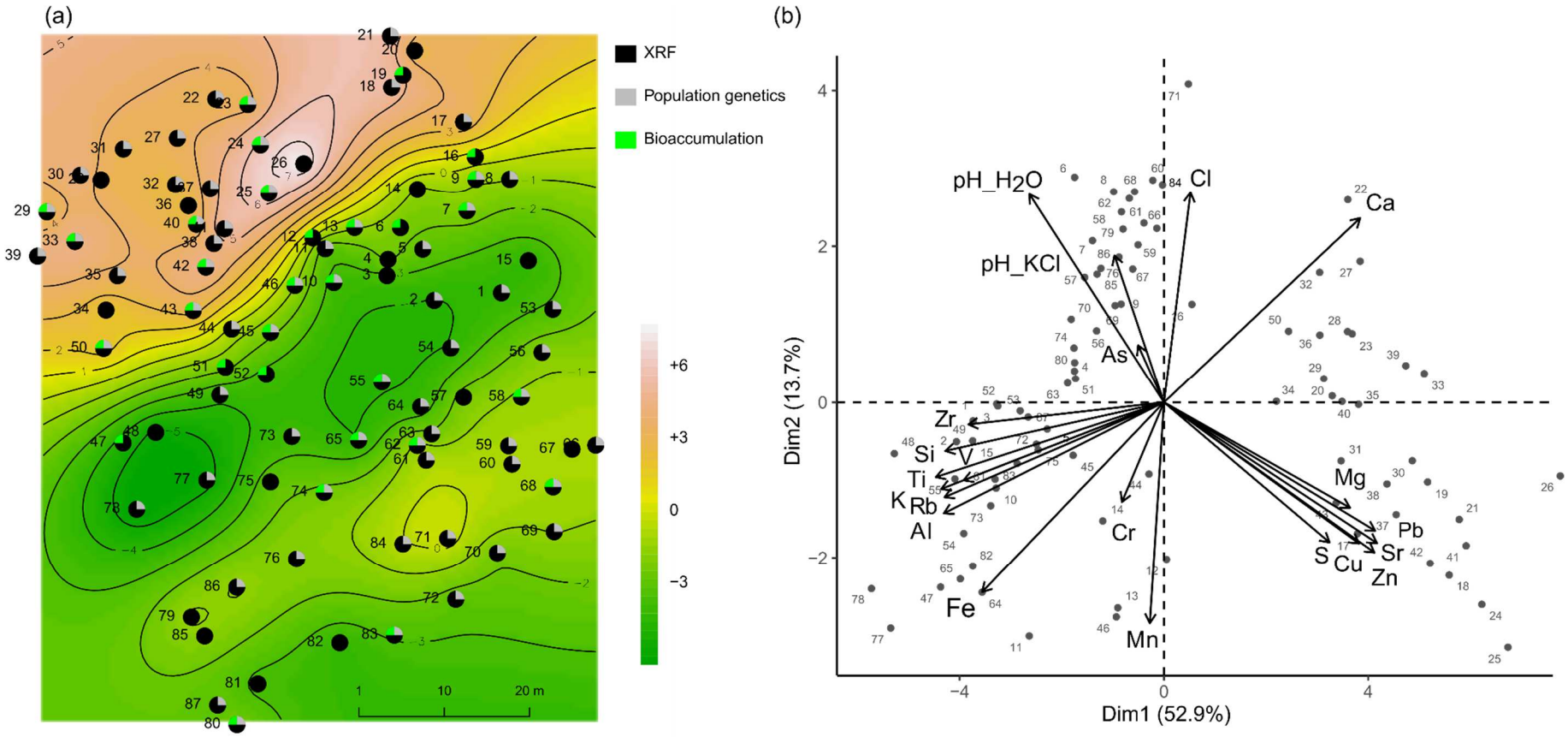
(a)
XRF
Population genetics
Bioaccumulation
+6
+3
0
−3
1
10
20 m
(b)
pH_H2O
pH_KCl
Cl
Ca
As
Zr
Si
V
Ti
K
Rb
Al
Fe
Cr
Mn
Mg
S
Cu
Pb
Sr
Zn
Dim1 (52.9%)
Dim2 (13.7%)

Figure 2

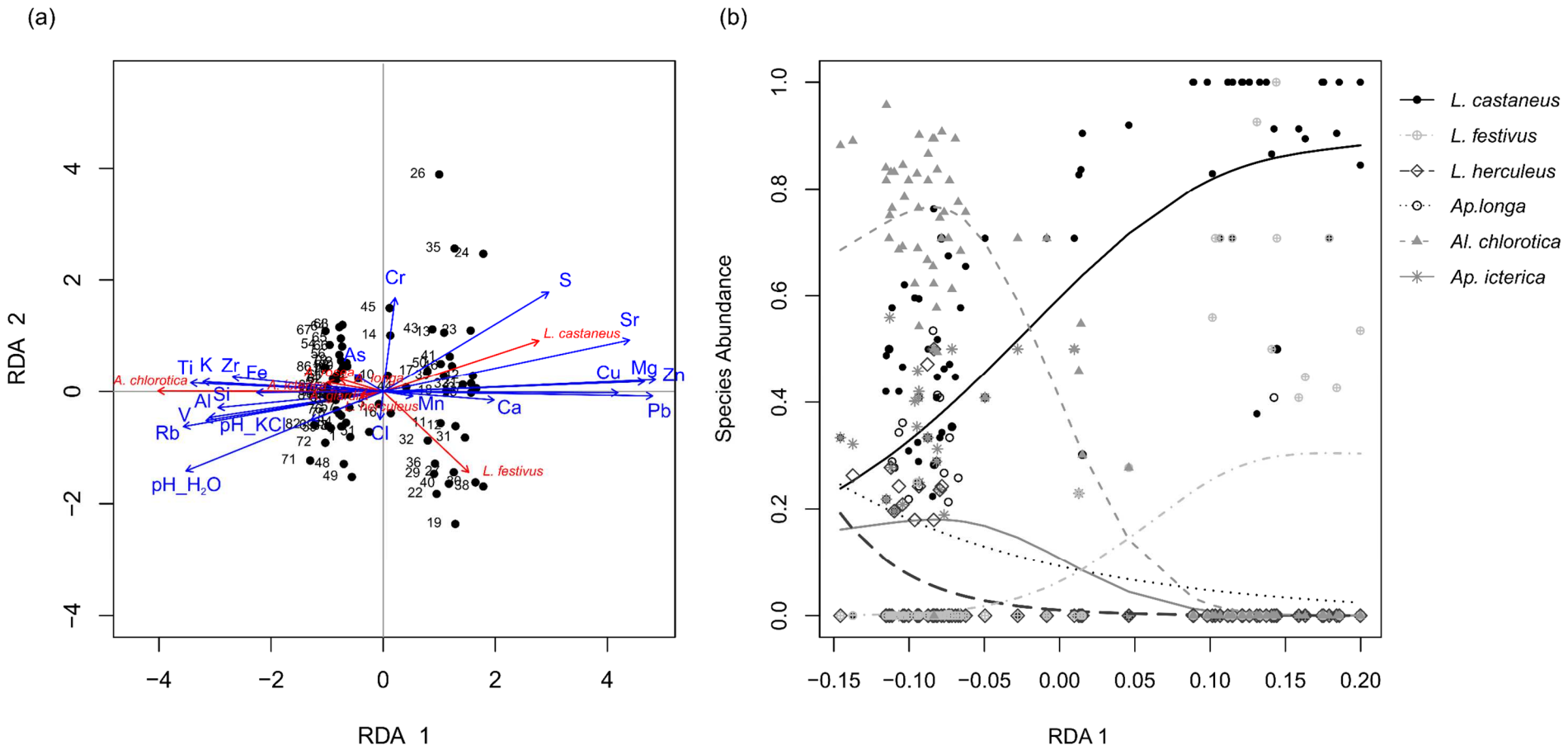
(a)
RDA 2
RDA 1
Cr
S
Sr
L. castaneus
Ti
K
Zr
Fe
As
A. chlorotica
Al
Si
V
Rb
pH_KCl
pH_H2O
Cl
Mn
Ca
Cu
Mg
Zn
Pb
L. festivus
(b)
Species Abundance
RDA 1
L. castaneus
L. festivus
L. herculeus
Ap.longa
Al. chlorotica
Ap. icterica

733 **Figure 3**

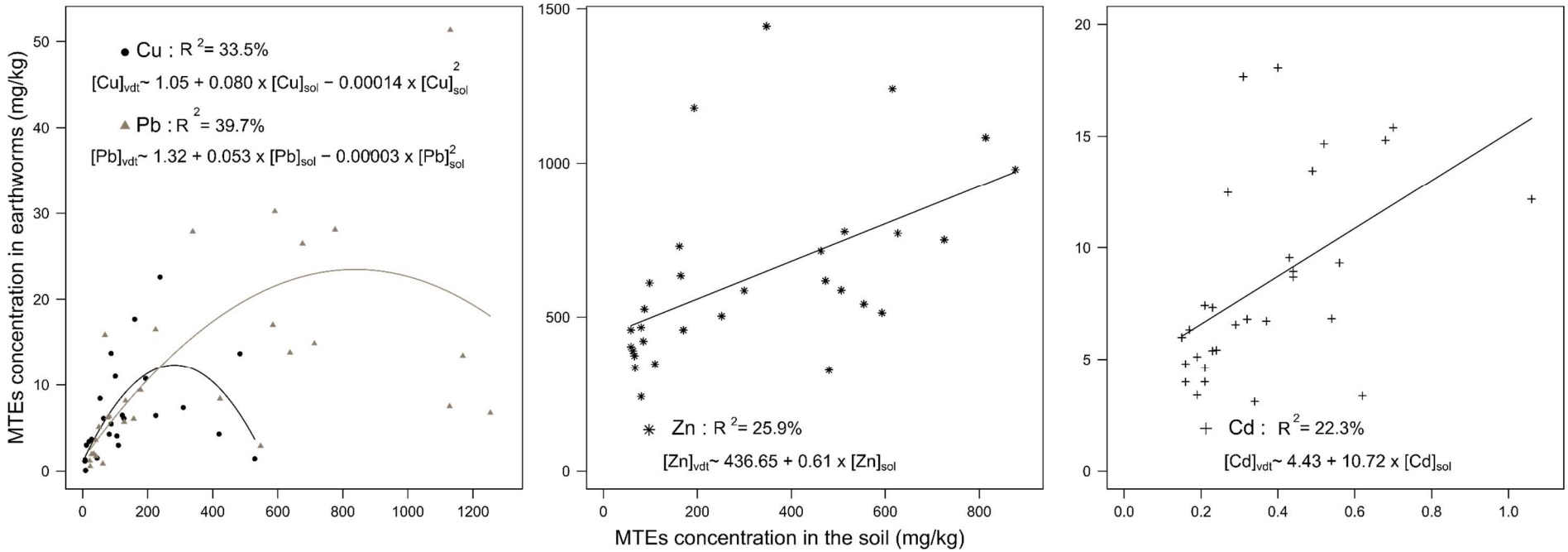

734
735

736 **Figure 4**

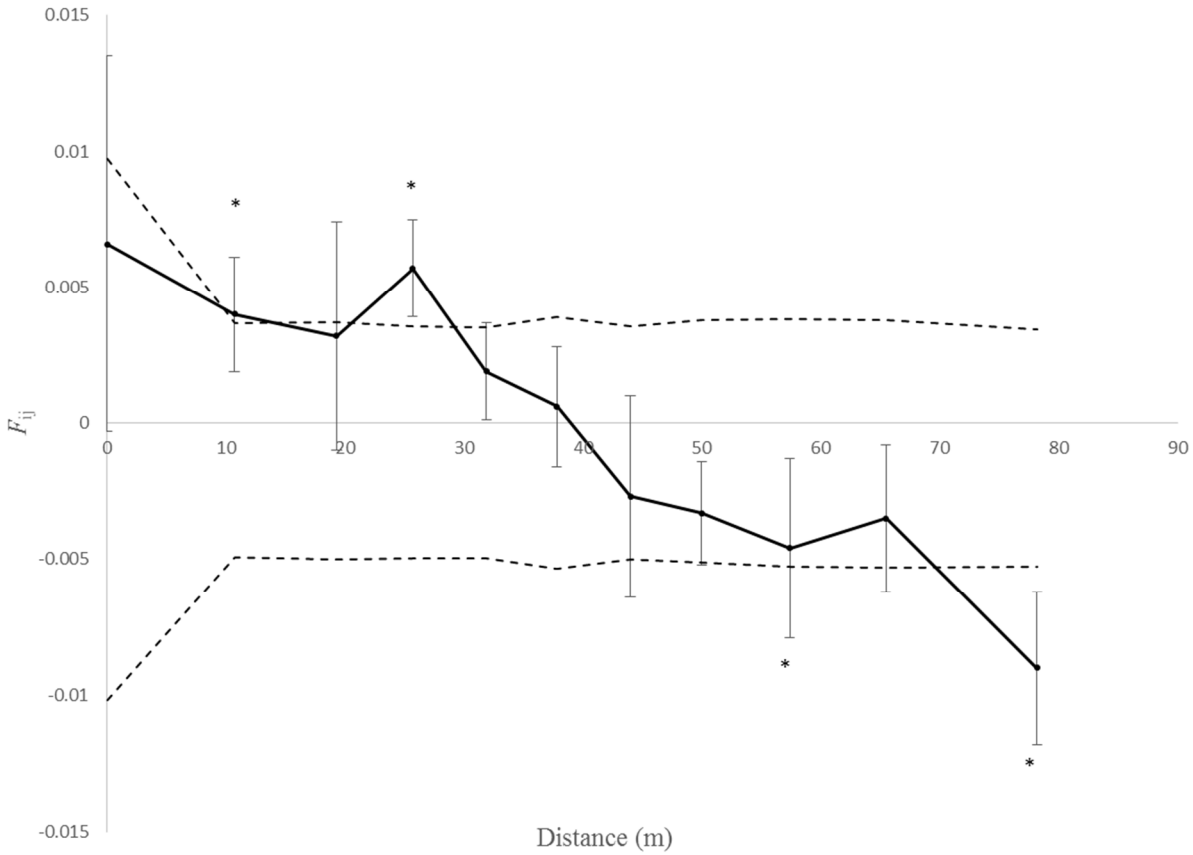

737

738 **Table 1 Characteristics of microsatellite data in the global dataset (175 genotypes) and in a subsample of one genotype per quadrat (63**
739 **genotypes). Are indicated: the number of alleles for each locus (Na), the estimator of the fixation index (F_{is}) with significant value in**
740 **bold, and the null-allele frequency (Null).**

Locus		**LC02**	**LC05**	**LC10**	**LC16**	**LC18**	**LC27**	**LC33**	**LC36**
175	N_a	5	10	18	36	22	10	10	19
genotypes	F_{is}	**0.184**	-0.081	**0.117**	**0.331**	**0.175**	-0.010	**0.239**	**0.334**
	Null	**0.096**	0.000	**0.057**	**0.162**	**0.082**	0.000	**0.118**	**0.164**
63	N_a	4	7	14	28	17	9	9	17
genotypes	F_{is}	0.118	-0.077	**0.166**	**0.362**	0.093	-0.098	**0.316**	**0.301**
	Null	0.000	0.000	**0.076**	**0.177**	0.000	0.000	**0.159**	**0.155**

741

742 **Appendix A**

743 **Table A1 Summary measures of the elemental composition and pH of the soil sampled. N corresponds to the number of quadrats in**
744 **which the element were found and quantified by XRF. The variance between repeated XRF-measures for a soil sample is given by the**
745 **minimum and maximum standard error ("min se" or "max se") for all measured soils. It corresponds to range of standard error found**
746 **when at least two replicated XRF measures report the element in a sample. Mean CV corresponds to the average coefficient of variation**
747 **found across measurements. Spatial autocorrelation across the study site was measure for each element using the Mantel test. Note that**
748 **Mantel tests for Ir, Nb, Th, Mo, Sb, Te, Os, Ta were not performed as the sample size for those element was too small (< 8).**

element	pH H_2O	pH KCl	S	Pb	K	Zn	Cr	As	Mg	Sr	V	Al	Zr	Ti	Rb	Ca	Si	Fe	Mn
min value (in pH unit and mass concentration in mg/kg)	6.41	6.42	57.0	14.0	1741.0	25.5	13.0	3.0	372.0	91.0	8.5	2826.5	46.0	581.5	21.0	43682.0	16030.0	7962.0	178.0
max (in pH unit and mass concentration in mg/kg)	7.87	7.45	7262.5	940.0	3534.0	638.5	85.0	18.5	2205.0	441.0	33.0	8192.0	129.0	1463.0	45.5	62140.0	31495.5	13324.0	246.7
mean (in pH unit and mass concentration in mg/kg)	7.28	7.24	651.3	214.5	2629.4	182.4	26.3	9.0	821.9	162.8	19.6	5202.2	81.4	1076.8	31.2	54107.9	24380.6	9932.1	206.5
sd (in pH unit and mass concentration in mg/kg)	0.27	0.18	1143.4	243.7	486.0	177.9	8.1	2.7	466.8	87.8	5.4	1103.5	16.5	209.4	5.6	4826.3	3403.6	1231.3	16.1
N	87	87	87	87	87	87	87	87	87	87	87	87	87	87	87	87	87	87	87
max/min ratio	1.23	1.16	127.4	67.1	2.0	25.0	6.5	6.2	5.9	4.8	3.9	2.9	2.8	2.5	2.2	1.4	2.0	1.7	1.4
min se	-	-	0.9	0.0	10.0	0.0	0.0	0.0	0.0	0.0	0.0	10.5	0.5	0.0	0.0	5.5	6.0	0.5	0.0
max se	-	-	307.5	76.5	352.7	116.5	30.0	8.5	134.0	98.0	9.0	886.0	15.0	530.5	4.0	1559.3	1847.0	854.0	40.0
mean CV (%)	-	-	26.1	6.5	6.3	7.9	15.8	52.5	3.2	5.7	16.4	11.3	8.9	6.7	5.3	0.9	3.7	2.5	7.6
Mantel test, p-value	0.03, p=0.23	0.005, p=0.43	0.06, p=0.15	0.44, p<0.001	0.19, p<0.001	0.40, p<0.001	0.015, p=0.37	0.04, p=0.14	0.44, p<0.001	0.26, p<0.001	0.18, p<0.001	0.16, p<0.001	0.14, p<0.001	0.25, p<0.001	0.27, p<0.001	0.04, p=0.12	0.16, p<0.001	0.11, p=0.004	0.06, p=0.052

749

element	Cl	Cu	Sn	P	Br	Y	Eu	Re	Hg	Ni	Ba	Yb	Ga	Ir	Nb	Th	Mo	Sb	Te	Os	Ta
min value (in pH unit and mass concentration in mg/kg)	1.5	9.0	27.0	6.0	2.0	5.0	1.0	2.0	1.0	6.0	56.0	0.0	0.5	0.5	4.0	1.0	1.0	27.0	27.0	8	3
max (in pH unit and mass concentration in mg/kg)	44.0	608.0	98.0	256.7	5.5	13.5	130.0	10.0	5.0	19.0	203.3	101.0	4.0	3.0	6.0	4.0	1.0	36.0	27.0	8	3
mean (in pH unit and mass concentration in mg/kg)	21.3	70.6	39.4	94.3	3.9	9.2	8.5	4.8	2.7	10.7	127.1	7.2	2.1	1.8	4.7	3.0	1.0	31.5	-	-	-
sd (in pH unit and mass concentration in mg/kg)	8.7	86.0	13.1	73.9	0.8	1.6	15.7	1.5	1.1	3.5	34.7	16.5	1.0	0.9	0.9	1.4	0.0	4.5	-	-	-
N	84	79	75	71	68	66	62	50	44	43	43	34	31	8	3	3	2	2	1	1	1
max/min ratio	29.3	67.6	3.6	42.8	2.8	2.7	130.0	5.0	5.0	3.2	3.6	-	8.0	6.0	1.5	4.0	1.0	1.3	-	-	-
min se	0.5	0.0	0.0	1.0	0.0	0.0	0.0	0.0	0.0	0.5	0.5	0.0	0.0	0.0	-	-	-	-	-	-	-
max se	23.0	437.0	26.5	29.5	1.0	1.0	126.0	3.5	1.5	6.5	21.0	99.0	1.0	0.6	-	-	-	-	-	-	-
mean CV (%)	42.6	11.2	9.6	22.9	8.6	5.1	27.3	39.3	38.1	31.9	6.8	46.1	37.5	63.8	-	-	-	-	-	-	-
Mantel test, p-value	0.06, p=0.054	0.25, p<0.001	0.26, p<0.001	0.40, p<0.001	0.15, p=0.007	0.18, p=0.001	-0.01, p=0.41	0.007, p=0.41	0.26, p<0.001	0.14, p=0.01	0.14, p=0.019	-0.035, p=0.47	0.31, p=0.001	-	-	-	-	-	-	-	-

750

751 **Table A2 Summary table of the GAM univariate models built for each species that showed a significant relationship between Hellinger-**

752 **transformed abundance data and RDA1.**

Model	Edf	Ref.df	F	p-value	Deviance explained (%)	Adj.R2
L. cataneus	1.75	1.94	35.01	<0.001	36.7	48.1
Ap. icterica	1.84	1.97	3.66	0.036	34.8	19.1
L. festivus	1.87	1.98	7.32	<0.001	45.5	28.2
L. herculeus	1.00	1.00	4.74	0.030	29.2	9.9
A. chlorotica	1.98	2.00	52.75	<0.001	90.3	86.0
A. longa	1.00	1.00	8.67	0.004	16.0	11.0

753

754 **Table A3. Analysis of deviance table (type II LR Chi-square tests) showing the effect of the soils score on PCA1 and PCA2 and of the**

755 **number of adults on juvenile abundances.**

756

# juveniles	df	Chisq	*p*
# adults	1	254.97	<0.001
PCA1	1	46.64	<0.001
PCA2	1	42.23	<0.001

757

Appendix B

The values of each quadrat on the first axis of the PCA (PCA1) were interpolated into a pollution map with a mesh size of 50cm (similar to the sampling size). To create this map of pollution we used the kriging interpolation method to account for spatial autocorrelation among points and used a Matern distribution to model variogram. The reliability of the interpolation map was checked through cross-validation of the residuals using 60 randomly selected points for the modelling set and 27 for the validation set. Note that we did not build such a map for the individual elements of particular interest in this study as they are all very much correlated to each other and to PCA1. Pearson correlation tests between Pb, Cu, and Zn, followed by Bonferroni correction for multiple testing showed that Pb and Cu were significantly correlated to Zn at 0.94 and 0.92, respectively. Cd was excluded as it was found in none of the soils analysed by XRF. All the above mentioned statistical analyses were done in R 3.6.1 (R core Team 2019) using gstat (Pebesma 2004, Gräler et al. 2016) and raster (Hijmans 2019) libraries.

References:

Pebesma EJ (2004) Multivariable geostatistics in S: the gstat package. Computers & Geosciences, 30: 683-691.

Gräler B, Pebesma E & Heuvelink G (2016) Spatio-Temporal Interpolation using gstat. The R Journal 8(1), 204-218

Hijmans RJ (2019). raster: Geographic Data Analysis and Modeling. R package version 2.9-5. https://CRAN.R-project.org